Analytical and Bioanalytical Chemistry
https://doi.org/10.1007/s00216-020-02824-0

RESEARCH PAPER

Ultrasensitive split-type electrochemical sensing platform for sensitive determination of organophosphorus pesticides based on MnO_2 nanoflower-electron mediator as a signal transduction system

Yuanfang Sun[1] · Pengyuan Xiong[1] · Juan Tang[1] · Zhiyao Zeng[1] · Dianping Tang[2]

Received: 22 June 2020 / Revised: 9 July 2020 / Accepted: 15 July 2020

Abstract

Organophosphorus pesticides (OPs) are extensively used worldwide as agrochemicals; however, excess use may threaten the health of humans. Thus, it is an urgent need to develop a sensitive method for determination of OPs. Herein, a simple and sensitive split-type electrochemical method was developed by using MnO_2 nanoflower-electron mediator as a signal transduction element. The MnO_2 nanoflower-electron mediator was synthesized and shows an excellent electrochemical signal attributed to the high specific surface area of MnO_2 nanoflower. Meanwhile, the inhibition of OPs on butyrylcholinesterase (BChE) was carried out in the homogeneous system. In the absence of target molecule, a large number of thiocholines (TCh) were yielded from hydrolysis of acetylthiocholine (ATCh) by BChE. The MnO_2 nanoflower was cracked, and subsequently, multiple electron mediator molecules were released from the platform after treated with TCh, thus decreasing the electrochemical response. Furthermore, the inhibition of OPs on BChE resulted in the reduced generation of TCh, thus inducing the recovery of electrochemical signal. Under the optimal experimental, dichlorvos can be detected in a wide range of 10^{-6}–10^{-10} M, with a detection limit of 3×10^{-10} M. Moreover, the assay was successfully used to analyze dichlorvos in cucumber juice and pear juice, showing a great promising potential for detecting organophosphorus pesticides in complex samples.

Keywords Organophosphorus pesticides · MnO_2 nanoflower · Split type · Electrochemical method

Introduction

The overuse of organophosphorus pesticides (OPs) has aroused serious problems in food safety and human health [1, 2]. OPs can inhibit the acetylcholinesterase activity even at low concentrations by the accumulation of acetylcholine in humans, which induced over-stimulated receptor in synapses and thus cause many diseases [2]. Therefore, it is urgent to design high efficiency methods for tracing of organophosphorus pesticide residues in foods. Classical analytical techniques such as mass spectrometry and liquid chromatography offer an excellent performance [3–5]. However, the high cost of instruments and the complicated labor requirement made it not suitable for rapid analyses. Thus, exploring for a simple and portable analytical method would be necessary.

Enzyme activity inhibition methods have emerged as the promising alternative for classical methods ascribed to the merits of rapidity and simplicity [6, 7]. In the enzyme inhibition system, the concentration of OPs was monitored by comparing the enzyme activity before and after reacted with target samples. Multiple analytical assays have been reported to measure the enzyme activity such as fluorescence assay, electrochemical assay, electrochemiluminescence assay, and colorimetric assay [8–12]. Among them, electrochemical-based enzyme inhibition assay has drawn considerable attention because of its obvious advantages like low budget, rapid operation, and high sensitivity [13, 14]. In the biosensing system,

Yuanfang Sun and Pengyuan Xiong contributed equally to this work.

✉ Juan Tang
Juan_tang@hotmail.com; tjhere@126.com

[1] Department of Chemistry and Chemical Engineering, Ministry of Education Key Laboratory of Functional Small Organic Molecule, Jiangxi Normal University, Nanchang 330022, Jiangxi, China

[2] Department of Chemistry, Key Laboratory of Analysis and Detection for Food Safety (Ministry of Education of China and Fujian Province), Fuzhou University, Fuzhou 350108, Fujian, China

Published online: 20 July 2020

most approaches were constructed based on an immobilized enzyme on the electrochemical transducer. Although these assays offer a high performance, the associated complicated steps for the preparation procedures and long analysis time are necessary. Moreover, the activity of the enzyme biomolecule could be weakened by conjugating with the nanomaterial or electrochemical material due to the harsh reaction condition [15]. Thus, the design of new signal transduction mode plays a vital role in improving the performance of the electrochemical biosensor.

A split-type biosensor, in which the biological reaction and the electrode reaction are separated in the different interfaces, seems like a good way to solve the problem of the traditional method [16, 17]. In the detection mode, an extra enzyme label conjunction step could be eliminated and the stable of the system can be highly improved. The key point of the design split-type biosensor is to explore an efficient and convenient signal amplified route. The MnO_2 nanoflower (NF) has gained increasing interest attributed to its intrinsic advantages including low toxicity and high specific surface area, which endows it an intriguing candidate for loading multiple electron mediators, e.g., thionine, ferrocene, and methylene blue [15]. Moreover, MnO_2 NF with the intermediate valence exhibited a strong oxidation ability and can be converted to Mn^{2+} by reducing substances, such as H_2O_2 and thiocholine (TCh) [18]. Thus, The MnO_2 NF–based nanomaterial can be used as an efficient electrode material for designing a high-performance split-type electrochemical biosensor.

Thus, a simple and sensitive split-type electrochemical method for the sensitive determination of organophosphorus pesticide (dichlorvos as an example) was fabricated by integrating the MnO_2-thionine signal-transducing material with an excellent enzyme inhibition effect by Ops. As designed, MnO_2-thionine heterostructure (MnO_2-Thi) was synthesized and applied as an electrochemical transducing material, which presents an excellent electrochemical response. When TCh (the enzymatic hydrolysate of acetylthiocholine by butyrylcholinesterase) transferred to the MnO_2-Thi based electrode, the current is significantly decreased due to dissolution of MnO_2. Interestingly, the electrochemical signal can be recovered by adding OPs to the BChE and ATCh system. The ingenious design offers a highly sensitive protocol for the determination of OPs.

Experimental

Material and chemicals

Potassium permanganate ($KMnO_4$), manganese sulfate monohydrate ($MnSO_4{\cdot}H_2O$), Nafion, and thionine acetate (Thi) were acquired from Aladdin (Shanghai, China). Acetylthiocholine (ATCh), butyrylcholinesterase (BChE), and dichlorvos (DDVP) were purchased from Sigma-Aldrich (St. Louis, MO, USA). All of the other reagents were of analytical grade and were used as received. Ultrapure deionized water (resistivity of 18.2 MΩ cm at 25 °C) was acquired from a Milli-Q water purification system (Millipore SAS Corporation, France).

Synthesis of the Thi-MnO_2 nanocomposite

Firstly, MnO_2 nanosheets were synthesized by consulting a previous study [19]. Generally, 1.0 g of $KMnO_4$ and 0.4 g $MnSO_4{\cdot}H_2O$ were initially added into 30 mL deionized water under continuous stirring to make it a homogeneous solution. Then, this solution was transferred to a 50-mL Teflon-lined stainless-steel autoclave and subjected to a reaction at 140 °C for 30 min. After cooling to room temperature, NFs were collected the by centrifugation at 9000 rpm (RCF average 5807 g-force) for 8 min, cleaned with ultrapure water and ethanol alternately. Lastly, the precipitates were dried at 70 °C for 6 h in an oven.

Next, the principle of positive and negative electrical attraction was applied to prepare the Thi-MnO_2 nanocomposite. Briefly, 2-mg MnO_2 NFs were dissolved in ultrapure water (2 mL) and added 1 mg Thi at room temperature for 24 h with gentle shaking. After this process, the obtained product was centrifuged at 8000 rpm (RCF average 4588 g-force) for 5 min and washed three times with ultrapure water as above. Finally, the precipitate was dispersed into 1 mL ultrapure water and stored in the dark at 4 °C for further use.

Construction of the sensor platform (Scheme 1)

A glassy carbon electrode (GCE) was repeatedly polished to a mirror shape with 0.05 and 0.03 μm alumina slurry, followed by successive sonication in ultrapure water and ethanol alternately for 3 min and dried in the air. After coated with 5 μL Nafion ethanol solution (v/v, 2%), the cleaned electrode was modified with 6 μL MnO_2-Thi dispersion and dried under a stream of air for 15 min. Subsequently, differential pulse voltammetry (DPV) was performed from − 0.2 to 0.35 V in 4 mL 0.1 M HAc-NaAc buffer solution (ABS) (pH 5.5).

Then, 15 μL of BChE (10 μg mL^{-1}, dispersed in pH = 7.4 ABS solution) and 15 μL different concentrations DDVP standard solutions were mixed at 37 °C for 30 min. Subsequently, 30 μL ATCh (10 mM) was added to react at 37 °C for 1 h.

After that, 10 μL of the above mixed solution of DDVP, BChE, and ATCh was incubated on the dried GCE for 30 min at room temperature; then, the electrode was washed gently with ultrapure water to remove the excess reaction fluid. Similarly, the second detection process was conducted by differential pulse voltammetry (DPV) at the same conditions.

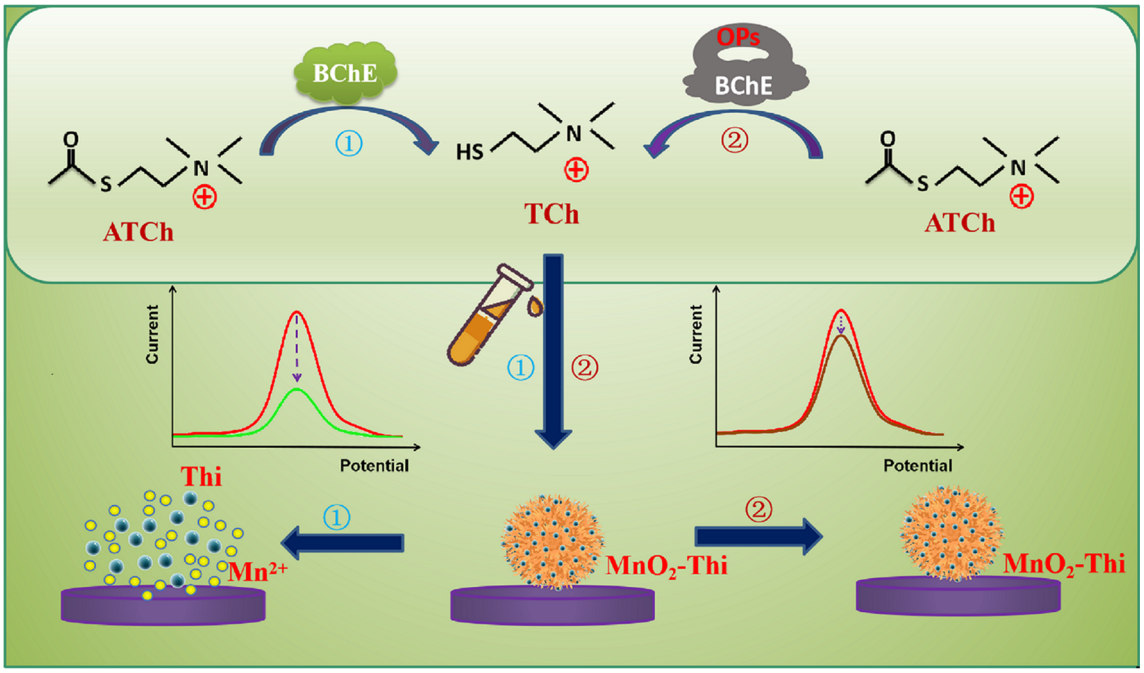

Scheme 1 Schematic illustration of the sensing system based on the MnO_2 nanoflower-Thi composite for OP determination

Results and discussion

Characterization of the MnO_2 nanoflower and MnO_2-Thi nanocomposite

The successful synthesis of the MnO_2-Thi nanocomposite is critical for the designed biosensor. The morphology of MnO_2 was characterized by a scanning electron microscope (SEM). Figure 1a illustrated that the MnO_2 nanoflowers were close spherical and uniform in size perfectly. And from Fig. 1b, the energy-dispersive spectrometry (EDS) confirmed that the elements Mn and O could be found. Moreover, it is clear that a large number of rod-shaped nanomaterials adhered to the surface of the MnO_2 nanoflower after the MnO_2 nanoflower was

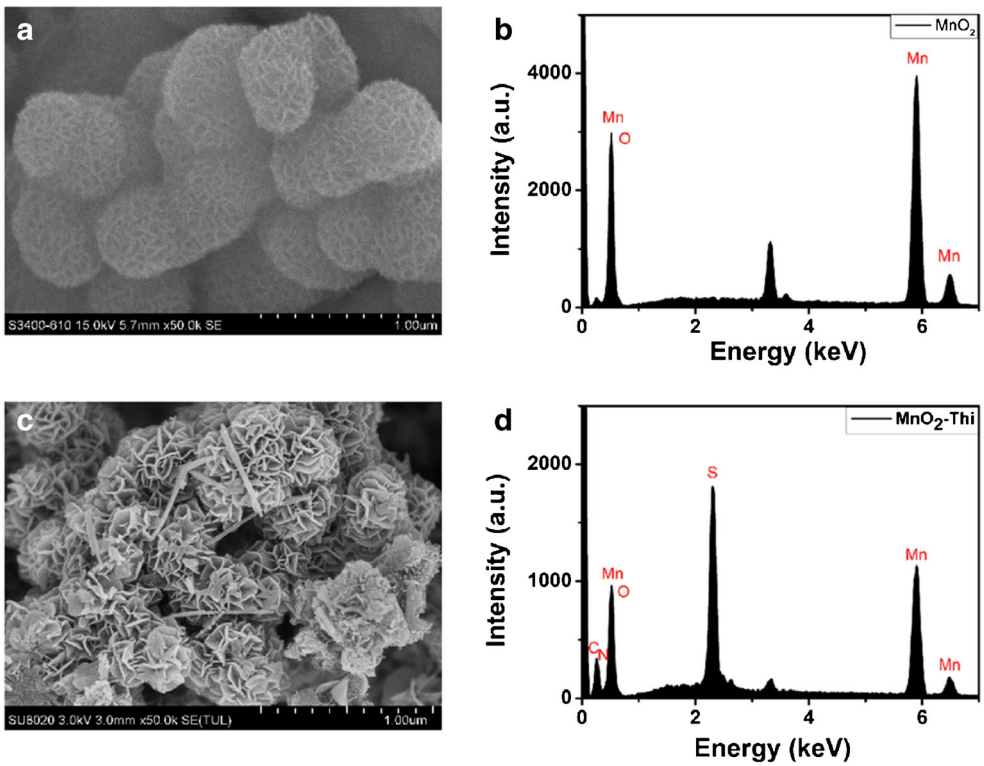

Fig. 1 SEM image (**a**) and EDS image (**b**) of MnO_2 nanosheets and SEM image (**c**) and EDS image (**d**) of the MnO_2-Thi nanocomposite

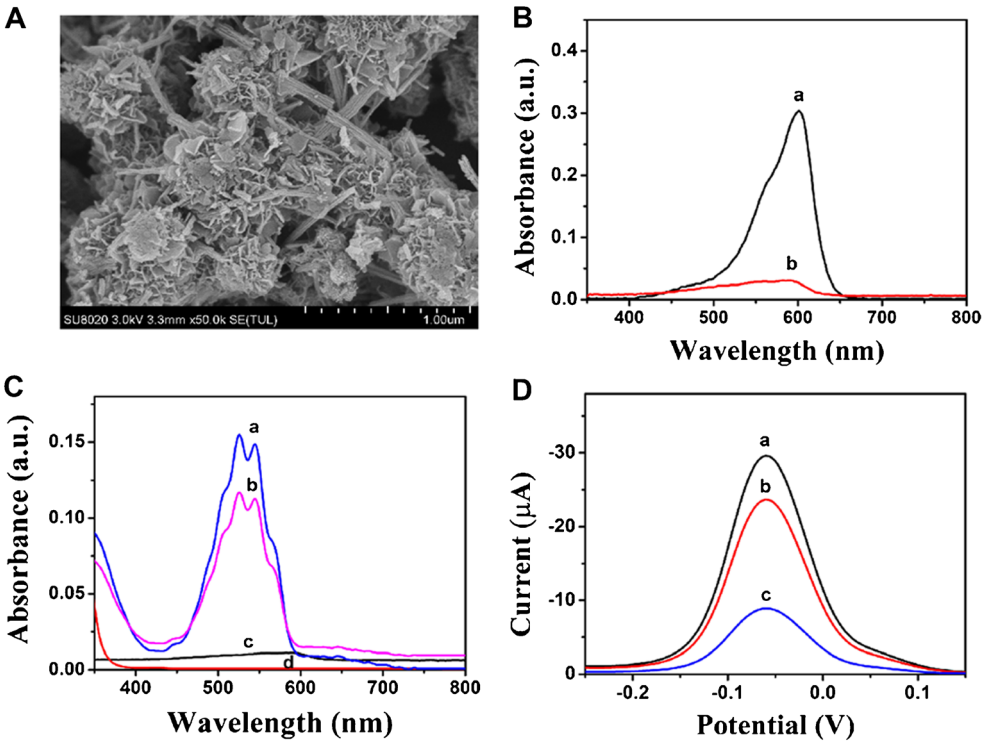

Fig. 2 **A** SEM image of the disintegrated MnO_2-Thi nanocomposite. **B** The UV-visible absorption spectra of the MnO_2-Thi nanocomposite before (a) and after (b) it was cracked. **C** The UV-visible absorption spectra of MnO_4^- (a), MnO_2-Thi nanocomposite + TCh + IO_4^- (b), MnO_2-Thi nanocomposite + TCh (c), and IO_4^- (d). **D** DPV of the MnO_2-Thi nanocomposite (a), MnO_2-Thi + ATCh + BChE + OPs (b), and MnO_2-Thi + ATCh + BChE (c)

decorated with Thi (Fig. 1c). The EDS results showed that all elements including Mn, O, C, H, N, and S were found in the nanocomposite (Fig. 1d). As shown above, it was revealed that the procedure for the synthesis of MnO_2-Thi was successful.

Design of the MnO_2-Thi sensor platform

As shown in Fig. 2A, the MnO_2-Thi nanocomposite is obviously reduced and the surface is sunken after mixed with TCh compared with that in Fig. 1C [20]. Furthermore, the UV-visible absorption spectrum was used to investigate that whether MnO_2-Thi can be destroyed by TCh. As illustrated in Fig. 2B, after the catalytic product TCh reacted with the nanocomposite, the absorption spectra of thionine sharply dropped. In addition, in Fig. 2C, the specific reaction between Mn^{2+} and IO_4^- was used to demonstrate the reduction product of the MnO_2-Thi nanocomposite. After the nanocomposite was mixed with ATCh, BChE, and IO_4^-, the characteristic UV-visible absorption spectra were well matched with that of MnO_4^- from 450 to 600 nm, indicating that the reduction product of the MnO_2-Thi nanocomposite was Mn^{2+}. Thus, all of the aforementioned results indicated the feasibility of this detection method using DDVP as the determination target.

Moreover, a question was aroused that whether the activity of BChE can be inhibited by dichlorvos. Thus, DPV measurement was performed. It can be seen that the electrical signal of the nanocomposite material was lower after treated with TCh (Fig. 2D), which is consistent with the UV-visible results. However, with the addition of the inhibitor dichlorvos, the activity of BChE decreased and less TCh was produced, resulting in a recovery of the electrical signal. These results

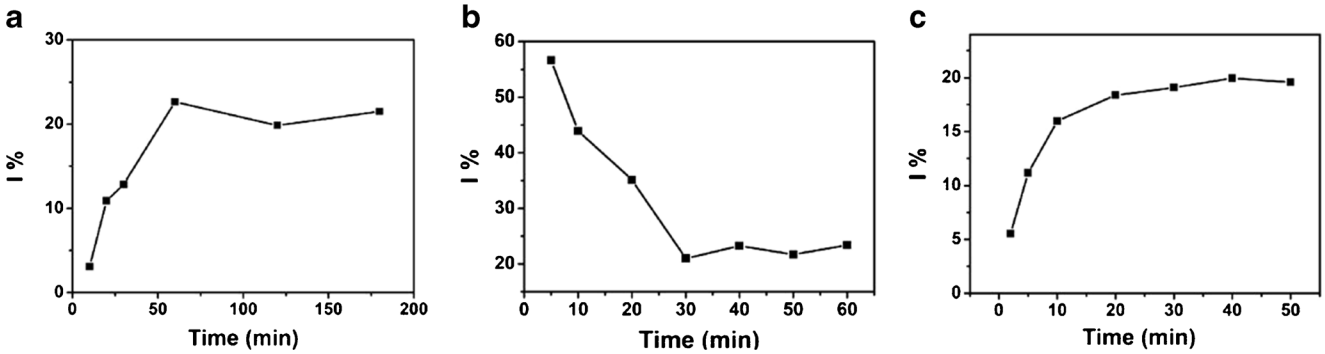

Fig. 3 Effect of **a** reaction time, **b** inhibitory time, and **c** incubation time

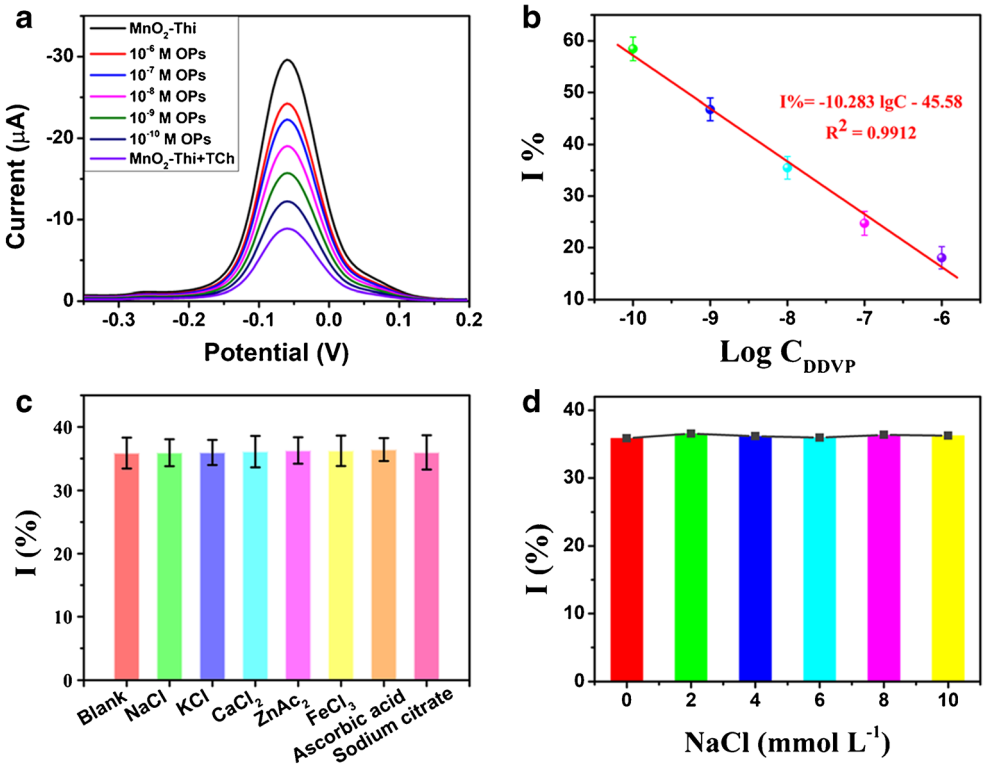

Fig. 4 **a** DPV of the different concentrations of DDVP with BChE/ATCh solution incubated on the MnO_2-Thi nanocomposite. **b** The relationship between inhibition rate and log C_{DDVP}; error bars represent the standard deviations of five independent measurements. **c** Effect of coexisting substances on the inhibition rate of DDVP; error bars represent the standard deviations of five independent measurements. **d** The effect of NaCl concentration on the inhibition rate of the BChE-ATCh-MnO_2-Thi system in the presence of 10^{-8} M DDVP

were adequately proved that the activity of BChE can be inhibited by dichlorvos.

Optimization of the determination conditions of DDVP

For enzyme activity sensors, the reaction time was strictly controlled in the determination experiment, such as the reaction time of ATCh and BChE, the reaction time of DDVP and BChE, and the incubation time of TCh with the MnO_2-Thi nanocomposite. All the evaluation was based on the inhibition rate by using 0.5 μM DDPV. I% was calculated by Eq. (1):

$$I\% = \frac{I_{\text{background}} - I_{\text{target}}}{I_{\text{background}}} \times 100\% \quad (1)$$

where $I_{\text{background}}$ and I_{target} are the current before and after MnO_2-Thi reacted with the mixture of DDVP, BChE, and ATCh.

As shown in Fig. 3a, the inhibition rate was increased with the increasing reaction time of ATCh and BChE, and attained a plateau after 60 min, indicating that TCh has reached its maximum concentration. To save experiment time, 60 min was selected as the reaction time. As seen from Fig. 3b, it is clear that the inhibition effect of DDVP was increased with the reaction time of BChE and DDVP. Therefore, the amount of produced TCh decreases, and the inhibition rate also be lower. A lowest rate was acquired at 30 min. Thus, 30 min was chosen as the optimal time. Figure 3c illustrates the relationship between inhibition rate and the incubation time of TCh on the MnO_2-Thi nanocomposite. With the increase of

Table 1 Comparison of different DDVP detection methods

Probe	Linear range (mol/L)	Detection limit (mol/L)	Reference
Electrochemistry	Not mentioned	4.2×10^{-9}	[22]
Fluorometry	4.5×10^{-9}–9.0×10^{-9}	4.3×10^{-9}	[23]
Fluorometry	4.49×10^{-9}–8.96×10^{-7}	4.49×10^{-9}	[24]
Electrochemistry	3.60×10^{-8}–2.26×10^{-5}	2.9×10^{-8}	[25]
Fluorometry	2.26×10^{-8}–1.36×10^{-6}	2.15×10^{-8}	[26]
Fluorometry	1×10^{-9}–1×10^{-3}	5×10^{-10}	[27]
Electrochemistry	4.5×10^{-7}–4.5×10^{-3}	3.0×10^{-7}	[28]
Electrochemistry	1×10^{-10}–1×10^{-6}	3×10^{-11}	This work

Table 2 DDVP determination results in real samples ($n = 3$)

Sample	Added (nM)	Measured (nM)	Recovery (%)	RSD (%, $n = 3$)
Cucumber juice	1.0	0.96	96	6.3
	10.0	10.13	101	4.8
	100.0	99.72	99.7	2.7
Pear juice	1.0	1.04	104	5.8
	10.0	9.87	98.7	4.3
	100.0	100.17	100	3.5

incubation time, more MnO_2 was reduced to Mn^{2+}, which made the Thi released from the platform electrode. So, the inhibition rate rose and reached its maximum value at 30 min. Therefore, 30 min is the best incubation time.

Dose–responses of sensitive detection toward DDVP

Under the optimum conditions, the analytical performance of the BChE-ATCh-MnO_2-Thi system was determined by using different DDVP standards. As shown in Fig. 4a, with the increase of DDVP, the inhibition rate was gradually decreased. And the inhibition rate has a good linear relationship with the concentration of DDVP within a dynamic working range from 0.1 nM to 1 μM (Fig. 4b). The regression equation could be fitted as $I\% = -10.283\lg C - 45.58$ and the correlation coefficient is $R^2 = 0.9912$. The limit of detection was estimated to 3×10^{-11} M.

The selectivity of the proposed DDVP detection method was further explored by adding various coexistence substances into the system. Figure 4c shows the interference effect of 10^5-fold for NaCl and KCl, 400-fold for $CaCl_2$ and Zn $(Ac)_2$, 200-fold for $FeCl_3$ and ascorbic acid, and 10^3-fold for sodium citrate on the determination of 1×10^{-8} M DDVP. It is obvious that commonly existed substances were hardly interfering. Thus, this method has high selectivity for the determination of DDVP [21].

Furthermore, salt tolerance is also one of the significant evaluation indicators of this electrochemical sensor. Thus, we studied the influence of NaCl on the sensing platform systematically. In Fig. 4d, it is obvious that the inhibition rate of the BChE-ATCh-MnO_2-Thi system has no apparent change in the different salt concentrations, proving that this system possesses an excellent salt tolerance ability and reliable stability. Notably, the obtained LOD of the system for DDVP detection is much lower than other reported methods (Table 1).

Detection of DDVP in the cucumber and pear juice samples

To further verify the practicality of the biosensor, different concentrations of DDVP in practical samples such as cucumber juice and pear juice were studied respectively [29, 30] (Table 2). It can be observed that the recoveries of the samples were in the range 96–104% and the RSDs were less than 7.0%. As a result, the system has a good performance in the accuracy, selectivity, and repeatability in practical sample detection than other methods [31].

Conclusions

In this assay, a split-type electrochemical biosensor was developed for the ultrasensitive determination of organophosphorus pesticides based on the MnO_2 nanoflower-electron mediator as an electrochemical signal component. The assay was constructed relying on the activity inhibition of butyrylcholinesterase by organophosphorus pesticides, in which dichlorvos was used as a model target. The process of activity inhibition of enzyme was performed in a homogeneous phase, which is separated from the electrochemical component, endowing the platform multiple merits such as avoiding of label and multiple complicated washing steps. In the presence of target, the electrochemical signal can be obviously recovered, which is related to the concentration of dichlorvos. Compared with other protocols for dichlorvos, the electrochemical split-type strategy presented great advantages in detection limit and linear range.

Funding information This work was financially supported by the National Natural Science Foundation of China (21864013) and the Open Project Program of Key Laboratory of Functional Small Organic Molecule, Ministry of Education, Jiangxi Normal University (No. KLFS-KF-201917).

Compliance with ethical standards

Conflict of interest The authors declare that they have no conflict of interest.

References

1. Liu X, Song M, Hou T, Li F. Label-free homogeneous electroanalytical platform for pesticide detection based on acetylcholinesterase-mediated DNA conformational switch

integrated with rolling circle amplification. ACS Sens. 2017;2(4):562–8.
2. Jokanovic M. Neurotoxic effects of organophosphorus pesticides and possible association with neurodegenerative diseases in man: a review. Toxicology. 2018;410:125–31.
3. Mol HGJ, van Dam RCJ, Steijger OM. Determination of polar organophosphorus pesticides in vegetables and fruits using liquid chromatography with tandem mass spectrometry: selection of extraction solvent. J Chromatogr A. 2003;1015(1–2):119–27.
4. Su R, Xu X, Wang X, Li D, Li X, Zhang H, et al. Determination of organophosphorus pesticides in peanut oil by dispersive solid phase extraction gas chromatography-mass spectrometry. J Chromatogr B Anal Technol Biomed Life Sci. 2011;879(30):3423–8.
5. Padrón Sanz C, Halko R, Sosa Ferrera Z, Santana Rodríguez JJ. Micellar extraction of organophosphorus pesticides and their determination by liquid chromatography. Anal Chim Acta. 2004;524(1–2):265–70.
6. Cao J, Wang M, Yu H, She Y, Cao Z, Ye J, et al. An overview on the mechanisms and applications of enzyme inhibition-based methods for determination of organophosphate and carbamate pesticides. J Agric Food Chem. 2020. https://doi.org/10.1021/acs.jafc.0c01962.
7. Hassani S, Momtaz S, Vakhshiteh F, Maghsoudi AS, Ganjali MR, Norouzi P, et al. Biosensors and their applications in detection of organophosphorus pesticides in the environment. Arch Toxicol. 2017;91(1):109–30.
8. Huang S, Yao J, Chu X, Liu Y, Xiao Q, Zhang Y. One-step facile synthesis of nitrogen-doped carbon dots: a ratiometric fluorescent probe for evaluation of acetylcholinesterase activity and detection of organophosphorus pesticides in tap water and food. J Agric Food Chem. 2019;67(40):11244–55.
9. Du D, Wang J, Wang L, Lu D, Smith JN, Timchalk C, et al. Magnetic electrochemical sensing platform for biomonitoring of exposure to organophosphorus pesticides and nerve agents based on simultaneous measurement of total enzyme amount and enzyme activity. Anal Chem. 2011;83(10):3770–7.
10. Chen H, Zhang H, Yuan R, Chen S. Novel double-potential electrochemiluminescence ratiometric strategy in enzyme-based inhibition biosensing for sensitive detection of organophosphorus pesticides. Anal Chem. 2017;89(5):2823–9.
11. Lu L, Xia Y. Enzymatic reaction modulated gold nanorod end-to-end self-assembly for ultrahigh sensitively colorimetric sensing of cholinesterase and organophosphate pesticides in human blood. Anal Chem. 2015;87(16):8584–91.
12. Zhang Q, Yu Y, Yun X, Luo B, Jiang H, Chen C, et al. Multicolor colorimetric sensor for detection of omethoate based on the inhibition of the enzyme-induced metallization of gold nanorods. ACS Appl Nano Mater. 2020;3:5212–9.
13. Dhull V, Gahlaut A, Dilbaghi N, Hooda V. Acetylcholinesterase biosensors for electrochemical detection of organophosphorus compounds: a review. Biochem Res Int. 2013;2013:731501.
14. Zhu C, Yang G, Li H, Du D, Lin Y. Electrochemical sensors and biosensors based on nanomaterials and nanostructures. Anal Chem. 2015;87(1):230–49.
15. Tang J, Huang Y, Zhang C, Liu H, Tang D. Amplified impedimetric immunosensor based on instant catalyst for sensitive determination of ochratoxin A. Biosens Bioelectron. 2016;86:386–92.
16. Tang J, Xiong P, Cheng Y, Chen Y, Peng S, Zhu ZQ. Enzymatic oxydate-triggered AgNPs etching: a novel signal-on photoelectrochemical immunosensing platform based on Ag@AgCl nanocubes loaded RGO plasmonic heterostructure. Biosens Bioelectron. 2019;130:125–31.
17. Shu J, Qiu Z, Zhou Q, Tang D. A chemiresistive thin-film translating biological recognition into electrical signals: an innovative signaling mode for contactless biosensing. Chem Commun (Camb). 2019;55(22):3262–5.
18. Lin Y, Zhou Q, Tang D, Niessner R, Knopp D. Signal-on photoelectrochemical immunoassay for Aflatoxin B1 based on enzymatic product-etching MnO_2 nanosheets for dissociation of carbon dots. Anal Chem. 2017;89(10):5637–45.
19. Aveiro LR, da Silva AGM, Antonin VS, Candido EG, Parreira LS, Geonmonond RS, et al. Carbon-supported MnO_2 nanoflowers: introducing oxygen vacancies for optimized volcano-type electrocatalytic activities towards H_2O_2 generation. Electrochim Acta. 2018;268:101–10.
20. Yan X, Song Y, Zhu C, Li H, Du D, Su X, et al. MnO_2 nanosheet-carbon dots sensing platform for sensitive detection of organophosphorus pesticides. Anal Chem. 2018;90(4):2618–24.
21. Hou J, Dong G, Tian Z, Lu J, Wang Q, Ai S, et al. A sensitive fluorescent sensor for selective determination of dichlorvos based on the recovered fluorescence of carbon dots-Cu(II) system. Food Chem. 2016;202:81–7.
22. Di Tuoro D, Portaccio M, Lepore M, Arduini F, Moscone D, Bencivenga U, et al. An acetylcholinesterase biosensor for determination of low concentrations of paraoxon and dichlorvos. New Biotechnol. 2011;29(1):132–8.
23. Huang N, Qin Y, Li M, Chen T, Lu M, Zhao J. A sensitive fluorescence assay of organophosphorus pesticides using acetylcholinesterase and copper-catalyzed click chemistry. Analyst. 2019;144(10):3436–41.
24. Meng X, Wei J, Ren X, Ren J, Tang F. A simple and sensitive fluorescence biosensor for detection of organophosphorus pesticides using H_2O_2-sensitive quantum dots/bi-enzyme. Biosens Bioelectron. 2013;47:402–7.
25. Cui HF, Wu WW, Li MM, Song X, Lv Y, Zhang TT. A highly stable acetylcholinesterase biosensor based on chitosan-TiO_2-graphene nanocomposites for detection of organophosphate pesticides. Biosens Bioelectron. 2018;99:223–9.
26. Yaneva M, Ivanov Y, Todorov N, Godjevargova T. Magnetic-nanoparticles-based fluorescent immunoassay for individual and simultaneous determination of dichlorvos and paraoxon in milk. Food Agric Immunol. 2017;29(1):228–43.
27. Hu Y, Li J, Li X. Leek-derived codoped carbon dots as efficient fluorescent probes for dichlorvos sensitive detection and cell multicolor imaging. Anal Bioanal Chem. 2019;411(29):7879–87.
28. Wei M, Wang J. A novel acetylcholinesterase biosensor based on ionic liquids-AuNPs-porous carbon composite matrix for detection of organophosphate pesticides. Sensors Actuators B Chem. 2015;211:290–6.
29. Lv S, Zhang K, Zhu L, Tang D. ZIF-8-assisted NaYF4:Yb, Tm@ZnO converter with exonuclease III-powered DNA walker for near-infrared light responsive biosensor. Anal Chem. 2020;92:1470–6.
30. Huang L, Chen J, Yu Z, Tang D. Self-powered temperature sensor with Seebeck effect transduction for photothermal-thermoelectric coupled immunoassay. Anal Chem. 2020;92:2809–14.
31. De Souza D, Machado SA. Electroanalytical method for determination of the pesticide dichlorvos using gold-disk microelectrodes. Anal Bioanal Chem. 2005;382(7):1720–5.